Preprint Title	Colorimetric detection of organophosphates with cysteamine capped gold nanoparticle sensors
Authors	Muhammad M. Shah, Wen Ren, Bashir Ahmad and Joseph Irudayaraj
Publication Date	04 Dec 2020
Article Type	Full Research Paper
Supporting Information File 1	OP_BJNANO_SupInfo_1st Dec,2020.docx; 266.4 KB
ORCID® iDs	Muhammad M. Shah - https://orcid.org/0000-0001-7319-5863; Bashir Ahmad - https://orcid.org/0000-0001-6047-3334; Joseph Irudayaraj - https://orcid.org/0000-0002-0630-1520

Colorimetric detection of organophosphates with cysteamine capped gold nanoparticle sensors

Muhammad Musaddiq Shah[1,2,3], Wen Ren[2,3], Bashir Ahmad[1] and Joseph Irudayaraj[*2,3,4]

[1] Department of Biological Sciences, International Islamic University Islamabad 44000, Pakistan

[2] Department of Bioengineering, University of Illinois at Urbana-Champaign, Urbana, IL, 61801, USA

[3] Biomedical Research Center, Mills Breast Cancer Institute, Carle Foundation Hospital, Urbana, IL, 61801, USA

[4] Micro and Nanotechnology Laboratory, University of Illinois at Urbana-Champaign, Urbana, IL, 61801, USA

*corresponding author

Running Title: A nanozyme sensor for colorimetric detection of neurotoxins

Abstract

Nanozyme biosensors have the potential to provide high sensitivity, multiple functionality, and tunable activity. A facile colorimetric biosensor for the detection of organophosphates (OPs) using cysteamine capped gold nanoparticle probes (C-AuNPs) as enzyme mimics is proposed. Parathion ethyl (PE) a class of OPs is a potent insecticide that functions by inhibiting the acetylcholinesterase (AChE) in the nervous system of insects. The inhibition kinetics of AChE using PE enables the development of a PE sensor. C-AuNPs possess the ability to catalyze the oxidization of 3, 3', 5, 5'-tetramethylbenzidine (TMB) to a blue-colored product without peroxidase. The detection of PE was monitored by the inability of AChE to generate choline. Choline causes the aggregation of C-AuNPs and the aggregated C-AuNPs has decreased ability to catalyze the oxidization of TMB. A calibration was developed in the 40-320 nM range for the quantitative detection of PE. The limit of detection observed was 20 nM and the method had excellent specificity. The proposed sensor provides an excellent platform for on-site monitoring of PE in environmental and food samples with high sensitivity and greater selectivity.

Keywords: colorimetric biosensor; cysteamine capped gold nanoparticles; nanozyme; neurotoxin; parathion ethyl

Introduction

Organophosphates (OPs) are one of the most applied insecticides in developing countries due to its low cost, wide availability, and high potency [1]. The residues of the OPs which have a long persistence in the natural environment pose a severe threat to terrestrial and aquatic animals [2]. According to the U.S. Environmental Protection Agency, OPs are highly toxic and hence categorized in the most toxic class " Class 1" [3, 4]. The presence of OPs leads to the malfunctioning of the central and peripheral nervous system by blocking the active site of acetylcholinesterase, AChE (EC 3.1.1.7), a prime functioning enzyme of the nervous system and the neurotransmitters. The enzyme controls the level of acetylcholine (ACh) by catalyzing it into choline and acetate at the synapse, which leads to the culmination of neurotransmission. Accumulation of ACh interferes with muscular functions, respiration, fluctuation in blood pressure, and myocardial abnormalities [5].

Detection of OP compounds has been traditionally performed with analytical methods such as gas chromatography (GC) [6], high-performance liquid chromatography (HPLC) [7], capillary electrophoresis [8], surface plasmon resonance [9], fluorimetry [10], and spectroscopic methods [11]. Although these techniques have been standardized, none of these methods are suitable for on-site monitoring and the rapid detection of OPs [12]. Biosensor based detection of neurotoxins has the potential to be simple, easy, rapid, cost-effective, portable, specific, and highly sensitive without the need for lengthy procedures [5].

Among these detection methods, enzyme-based biosensors can be a better substitute for the detection of insecticides and pesticides including OP because these toxins are enriched with compounds that can block the diverse enzymes of insects and pests [13], including AChE.

To generate a signal for on-site detection, oxidase mimicking materials such as MnO_2 nanosheets and surface-modified cerium oxide nanoparticles have been used for the signal in colorimetric methods via TMB oxidation [14, 15]. TMB, nanozymes, and hydrogen peroxide (H_2O_2) based colorimetric detection systems are already being employed by different research groups [16-18]. The term "nanozyme" was coined 1st time to describe gold nanoparticles possessing the capability of transphosphorylation [19]. Nanozymes are those nanomaterials that are capable to mimic the functions of enzymes. As these easy-to-synthesize materials showed higher stability compared to proteins under harsh conditions so their applications are increasing in different fields especially in

biomedical and sensing applications [20, 21]. Huang et al. divided these enzyme mimic materials into two classes, e.g., oxidoreductases and hydrolases [22]. Colorimetric nanozyme based biosensing methods for OPs are simple, cheap, easy to develop approaches because of its capability in on-site monitoring of these compounds with signal for naked eyes without requirement on readout instrument.

Herein, we capitalize on the enzyme mimic capabilities of C-AuNPs to develop a biosensor for rapid and sensitive detection of PE. C-AuNPs was used to catalyze the oxidization of TMB to produce a colorimetric blue product. The presence of PE in the system would block the enzymatic potential of AChE, which causes the suppression of choline production and induced less aggregation of C-AuNPs. The monomers of C-AuNPs exhibited strong catalytic activity for the oxidization of TMB, resulting in the production of blue color. This peroxidase-like activity is exploited to detect the presence of PE in a given sample. When the inhibitor, target PE is absent, acetylcholine chloride will be hydrolyzed, catalyzed by AChE, resulting in choline production. Choline induces aggregation in C-AuNPs and aggregated C-AuNPs could not catalyze the oxidization of TMB, the obtained solution was colorless. The intensity of the bluish color of the oxidized product is directly proportional to the concentration of the target PE and vice versa. The principle of our detection mechanism is illustrated below in Scheme 1.
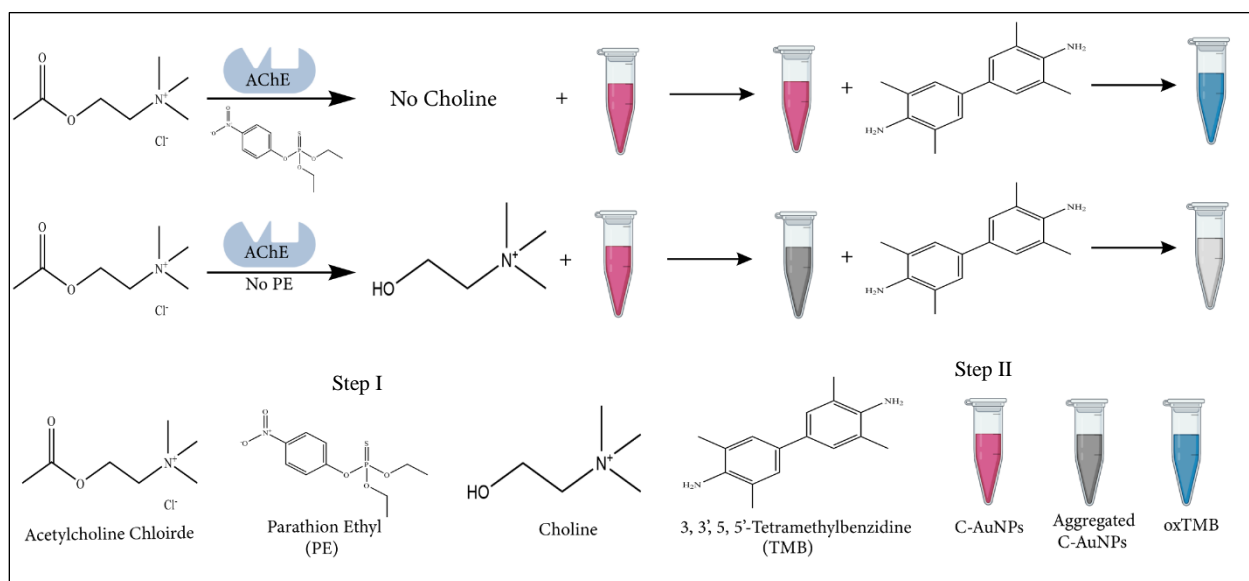
Scheme 1: Schematic representation of colorimetric detection of organophosphates via C-AuNPs. Step 1 represents the effect of PE on the formation of choline. Step 2 represents the oxidation power of dispersed and aggregated C-AuNPs.

Results and discussion

Characterization of cysteamine capped AuNPs

The characterization of the C-AuNPs, including physical (shape, size), chemical (surface charge), and optical (absorptivity) features, were studied (Figure 1). The UV-visible absorbance spectra showed a typical sharp peak at 530 nm for the C-AuNPs due to the strong surface plasmon resonance (SPR) of these plasmonic nanoparticles. The peak indicated that the average size of these nanoparticles is in this range between 30-40 nm. The hydrodynamic radius of these nanoparticles as evaluated by DLS was 33 nm. A high positive surface charge (+39.4 ± 2.05 mV) not only confirms the stability of these nanoparticles but also indicates the presence of amine groups on the surface of these nanoparticles.

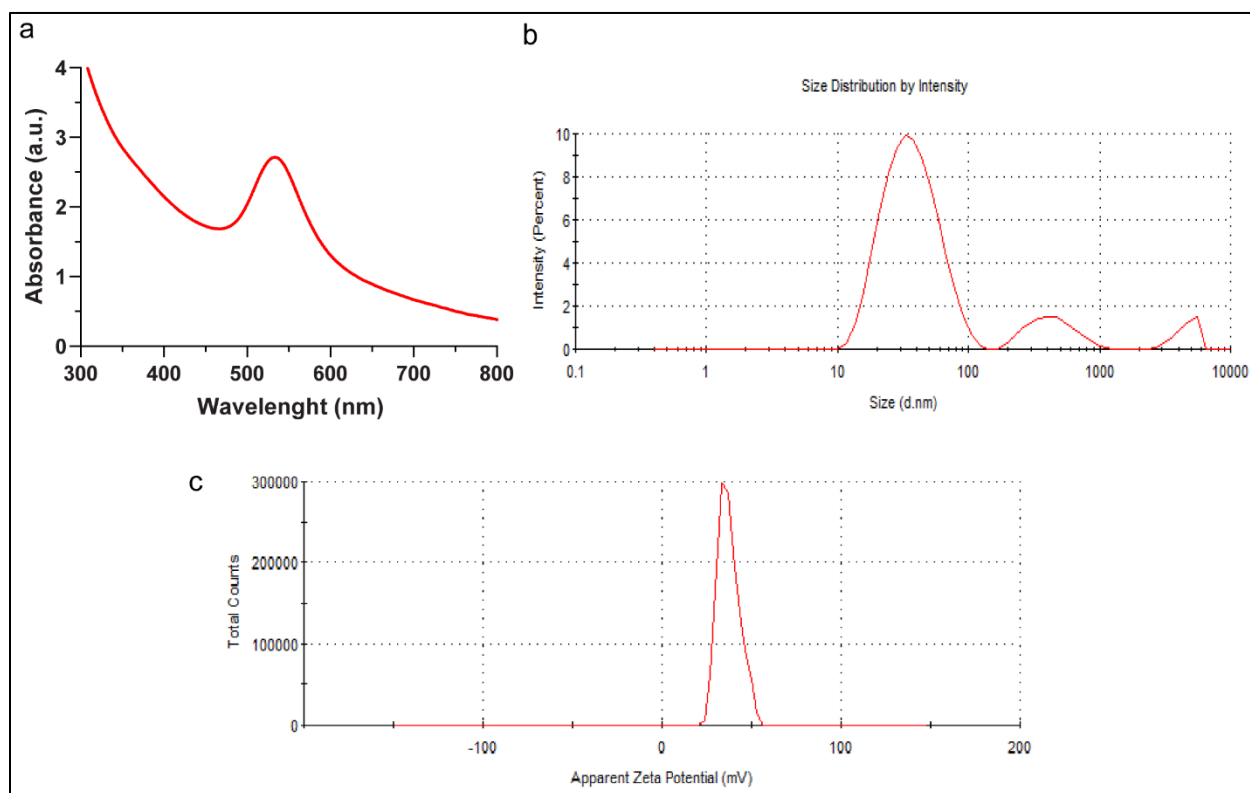**Figure 1:** Characterization of C-AuNPs. (a) UV-visible spectrum (b) Dynamic Light Scattering (c) Zeta Potential

Optimization of reagents and reactions

The AChE maximally hydrolyzed ACh (4.0 mmol·L^{-1}) after incubating for 20 minutes with Tris HCl buffer 7.6 as a reaction medium (Sec. SI.1). The 100 pM of C-AuNPs best oxidized the 0.4 mmol·L^{-1} TMB in acetate medium (pH 4.0) (Sec. SI.2).

Instantaneous oxidation of TMB by C-AuNPs

The peroxidase-like activity of C-AuNPs and the adverse effect of choline on the catalytic activity of these nanoparticles were studied with TMB as a typical peroxidase substrate [23]. Figure 2a expresses the peak of C-AuNPs with a maximum at 530 nm (red spectra). The aqua color peak represents the UV-vis spectra of colorless TMB, but when C-AuNPs were incubated with TMB, in presence of H_2O_2 they catalyzed the oxidation of the TMB within 60 seconds of reaction at room temperature. Two sharp peaks, 370 nm, and 652 nm, and intense blue colors confirm the oxidation with C-AuNPs, which renders it a nanozyme (dark blue spectra) [24].

Figure 2b confirms the adverse effects of choline on the catalytic activity of C-AuNPs. This aggregation effect is observed not only by the reduction in the color of the enzymatic product but also by the UV-Vis spectra without any prominent peaks. The aggregation of C-AuNPs due to the presence of choline has also been reported by El et al. [25]. The reason behind this aggregation is depending upon the deprotonation of cysteamine under the influence of pH. Amine groups of C-AuNPs are being deprotonated at alkaline pH [26]. The positively charged choline acts as a bridge among deprotonated C-AuNPs and leads to the aggregation of these nanoparticles. The aggregated form of C-AuNPs loses its catalytic activity and unable to catalyze the oxidization of TMB. Depending upon the pH of the medium cysteamine exists in three ionic forms: the positively charged form (cys+), the zwitterionic form (cys-ZW), and the negatively charged form (cys-) [27]. The presence of OPs in the reaction mixture reduced the hydrolysis of ACh, thus less influence on the catalytic activity of C-AuNPs.

According to Figure 2c, the presence of both AChE and ACh leads to choline production, which causes aggregation and ultimately, a reduction in the catalytic activity of C-AuNPs. The inset represents the corresponding colors. Results obtained confirm that C-AuNPs have a catalytic activity to generate a colorimetric signal with TMB. PE presence causes less hydrolysis of ACh which consequently produces less choline, less choline indicates lesser aggregation of C-AuNPs which ultimately produces a strong catalytic activity to produce brighter colorimetric signals.
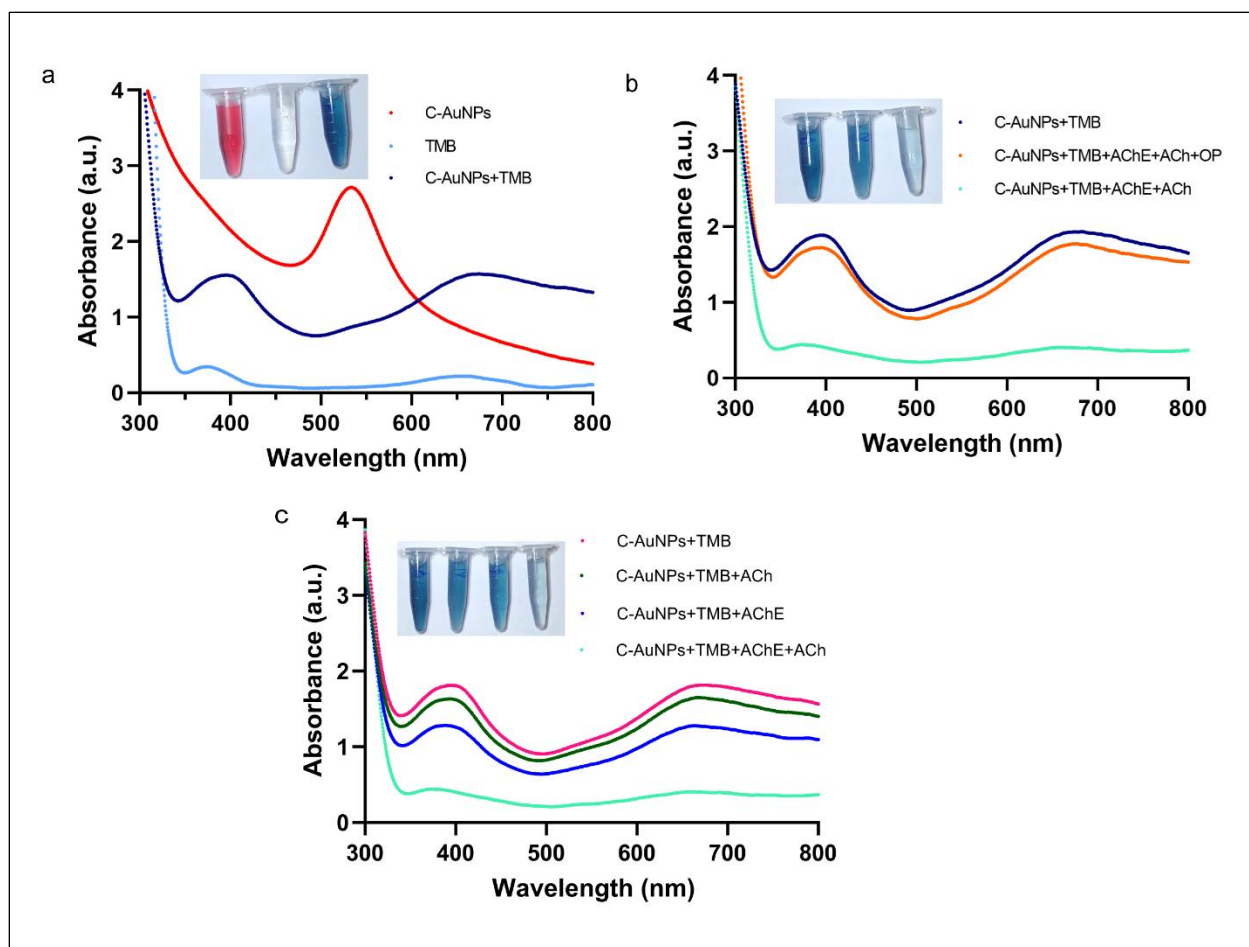
Figure 2: Nanozymic nature of C-AuNPs, effected by PE and choline on the oxidation of TMB. (a) The UV-Vis absorption spectra of C-AuNPs, TMB, and C-AuNPs+TMB confirm the formation of oxTMB. (b) The difference in UV-vis spectra in the presence and absence of PE confirms choline production, which leads to the reduction in the catalytic activity of C-AuNPs. (c) UV-Vis absorption spectra confirm that the formation of choline due to AChE and ACh ultimately causes the aggregation of C-AuNPs.

Detection of PE

The AChE activity was inhibited when PE was incubated with AChE. After that ACh, C-AuNPs, and TMB were added to this reaction mixture. Consequently, a suppressed amount of choline was produced. With an increase in the concentration of PE, a gradual inhibition pattern was observed, and hence higher oxidation of TMB along with an obvious blue color [28] (Figure 3). Irreversible inhibition of AChE has already been reported due to the presence of OPs [29, 30]. The formation of a covalent bond with the active site (phosphorylate serine residues) of AChE by these toxic chemicals converts the enzyme into a non-functioning molecule [31].
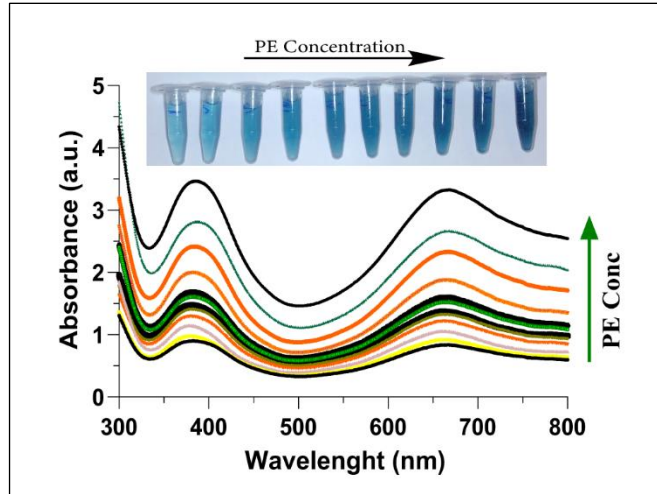
Figure 3: UV-Vis absorption spectra of AChE+ACh+C-AuNPs+TMB plotted with increasing concentrations of PE (0-400 nM). The increase in PE concentration leads to less aggregation of C-AuNPs thus a stronger catalyzed colorimetric reaction with deeper color from oxTMB. The inset shows the color of the corresponding reaction mixtures.

C-AuNPs concentration and oxTMB

While evaluating the correlation between concentrations of C-AuNP and oxidation of TMB, a direct relationship was noted between nanoparticle concentrations and oxTMB. Higher the concentration of C-AuNPs, higher the absorbance of oxTMB as observed for the dilutions of C-AuNPs from 10 pM to 120 pM. The UV-Vis spectra in Figure 4 show a direct relationship between C-AuNPs and oxTMB.
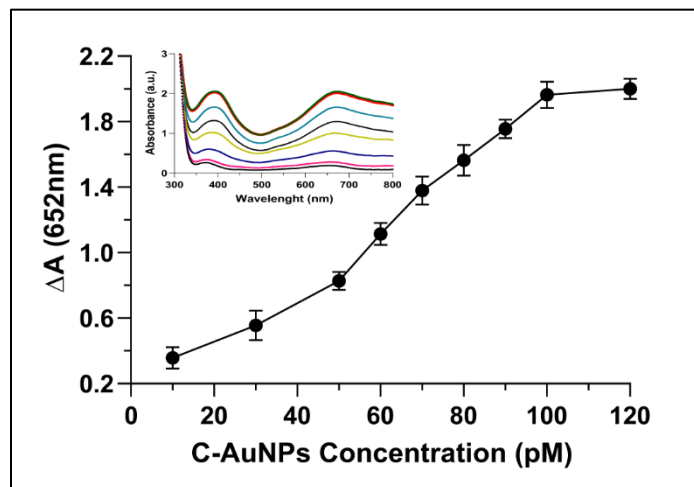

Figure 4: UV-Vis absorption spectra illustrate the catalytic activity of C-AuNP in different concentrations. Inset represents the UV-Vis spectra of C-AuNPs and TMB with increasing concentrations of C-AuNPs.

The inhibition efficiency

The inhibition efficiency (IE%) of AChE was detectable in the tested range between 20 and 400 nM concentrations as shown in Figure 5a. The inhibitor showed a linear correlation in the range between 40 and 320 nM, which is in agreement with the previously described methods [14, 32]. The IE% was calculated using the formula noted in the supplementary information (Sec. SI.3). The limit of detection of this assay is 20 nM, which is better than several previous reports [33-36]. According to the Codex Alimentarius (FAO-WHO) database [37] maximum residual limit for parathion in spices and fruits should not exceed 200 ng·mL^{-1} (0.2 mg·kg^{-1}). The biosensor developed in our work can detect PE as low as 5.8 ng·mL^{-1} (20 nM), which advocates for the high sensitivity of this assay. Thus, our proposed sensor meets the detection requirements for on-site and robust visual detection of OPs colorimetry with high sensitivity.

Selectivity assay

Cross-reactivity of the designed probe was evaluated utilizing recent environmental contaminants and cancer-causing agents (imidazole, PFOS, and PFOA) which were introduced at a concentration as high as 100 nM instead of PE (100 nM). None of these chemicals induced the same colorimetric response. Our results indicated that the probe is specific enough to detect the PE selectively with high precision and reliability, as shown in Figure 5b.

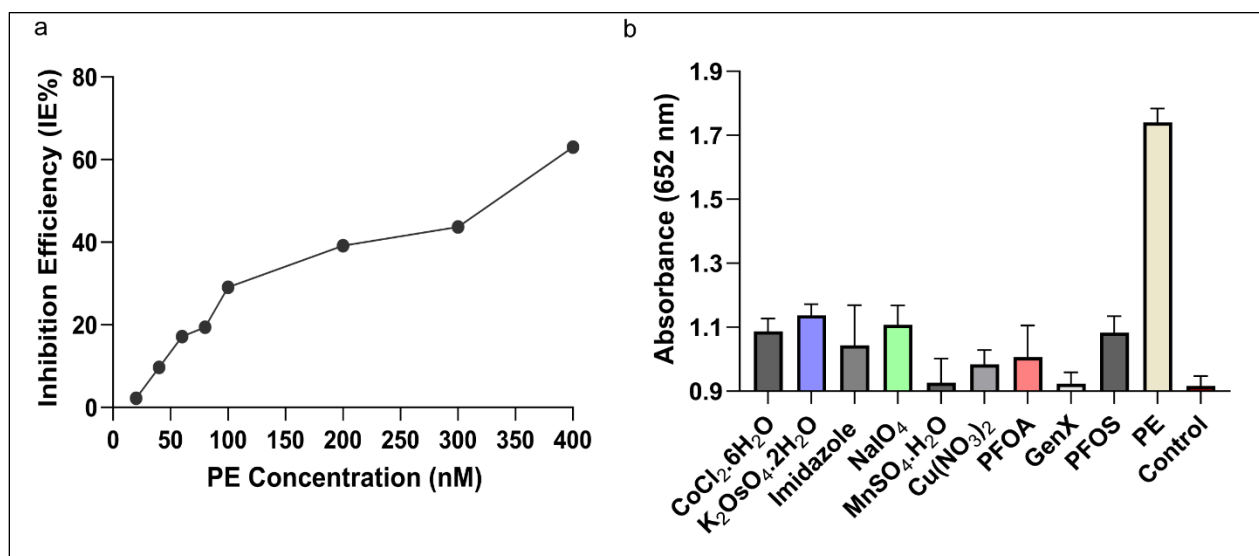**Figure 5:** Inhibition efficiency and Specificity of the assay. (a) Inhibition efficiency of PE on AChE activity. The inhibition of AChE enhanced with increasing concentrations of PE. (b) The selectivity of the developed assay towards PE, carcinogenic compounds, and other toxins at a wavelength of 652 nm. The absorbance of PE was much higher compared to the other compounds tested.

Comparison of different OPs monitoring systems

A comparison of our work with other reported methods for the detection of OPs is summarized in Table 1. Compared to sensor technologies that utilize parathion-methyl as an analyte, our approach exhibited 180 times better sensitivity compared to the MPH enzyme-based biosensor [34] and 3 times better than the QD-based sensor [33]. The sensitivity achieved is comparable to the sensitivity of Fe_3O_4 imprinted polymers [38] and overall, the assay developed was simple, more sensitive, and was highly selective in detecting OPs.

Table 1: Comparison of different OP detection systems

	Method	Linear Range ng·mL⁻¹	LOD ng·mL⁻¹	Target Analyte	References
1	LC-MS	--	0.5	Glyphosate	[39]
2	Enzyme-linked immunosorbent assay	0.44-8.48	0.19	Parathion	[40]
3	3QD based sensor	25-3000	18.0	Parathion-Methyl	[33]
4	Biosensor using MPH enzyme	0-26,312	1052.8	Parathion-Methyl	[34]
5	Fe_3O_4 imprinted polymers	15-2500	5.2	Parathion-Methyl	[38]
6	MIP-B-TiO2 NRs-Voltammetry	0.01-100	7.4×10^{-3}	Chlorpyrifos	[41]
7	Fluorometric and colorimetric	0.125–750	0.125	Carbaryl	[42]
8	AChE/AuNPs based system	0.01-1.0	2.78×10^{-5}	Malathion	[43]
9	RB-AuNPs based system	969.2–3632.5	8.965	Ethoprophos	[35]
10	Aptamer-AuNPs	21.31-2130	2.1×10^7	Omethoate	[36]
11	**Colorimetric nanoenzyme sensor**	**11.65-93.2**	**5.8**	**Parathion-Ethyl**	**Our study**

Conclusion

Herein, we developed a simple and sensitive sensor technology for the detection of PE, a typical chemical of the neurotoxin organophosphates by colorimetry. The biosensor utilizes C-AuNP to catalyze the oxidization of the colorless TMB into a blue-colored reagent for visual monitoring of PE with excellent specificity well below the maximum contaminant level prescribed by the FAO-

WHO. A calibration was developed in the linear range between 40 and 320 nm and a detection limit of 20 nM was observed with a cost-effective and simple methodology. The peroxidase-free colorimetric detection system can be utilized in a range of applications to monitor PE in environmental and food samples, such as irrigation water, juices, milk products, fruit and vegetable wash for quality control, and safety purposes.

Experimental

Materials and reagents

All chemicals used in this work were of analytical grade as received. Acetylcholinesterase (AChE, from electrophorus electricus), acetylcholine chloride (ACh), gold salt (HAuCl$_4$.3H$_2$O), and PE were purchased from Sigma Aldrich USA. TMB was obtained from MOSS Inc. USA. Stock solution (0.5 U·mL^{-1}) and working solution (2.0 m U·mL^{-1}) of AChE were prepared using 20 mM Tris–HCl buffer (pH 7.5). Standard and working solutions of HAuCl$_4$.3H$_2$O, cysteamine, sodium borohydride (NaBH$_4$), and 4.0 mmol·L^{-1} ACh working solution were made using Milli Q water (18.25 MΩ·cm) in volumetric flasks. The working solution of 0.4 mmol·L^{-1} of TMB was prepared in 100 mM sodium acetate buffer (pH 4.0) and different dilutions of PE (20, 40, 60, 80, 100, 200, 300, and 400 nM) were prepared using ethyl alcohol (95%). All of the solutions and dilutions prepared were kept at 4°C until further use.

Instrumentation

Absorption measurements were performed with Nanodrop UV-Vis Spectrophotometer (Thermo Scientific, Loughborough, U.K.). Dynamic Light Scattering (DLS) and Surface charge density (Zeta potential) were measured with a zeta sizer (Malvern Zetasizer, Nano ZS-90, U.K.).

Synthesis of C-AuNPs

The method used for the synthesis of C-AuNPs was adapted from Ren et al. [44] with necessary modifications. Briefly, 1.42 mM solution (40 mL) of HAuCl$_4$.3H$_2$O was sonicated and mixed with 400 µL of cysteamine solution at a concentration of 213 mM, followed by continuous stirring at 500 rpm for 20 minutes in an amber flask. A capping solution consisting of 10 mM (10 µL) NaBH$_4$, was added and kept at constant stirring for an additional 30 minutes at room temperature. To remove the unreacted species and unbound cysteamine ligands from colloidal C-AuNPs, the

solution was centrifuged at 12000 rpm at room temperature for 20 minutes, the supernatant was removed, and the pellet was resuspended in Milli Q water (18.25 MΩ· cm). UV-vis is not only being applied to confirm the C-AuNPs but also used to determine the size as well as the concentration of these nanoparticles [45]. After that, the colloidal solution was stored at 4°C to avoid further aggregation.

Optimization

The factors involved in enzymatic hydrolysis of ACh and the chromogenic reaction (oxidation) of TMB by C-AuNPs were optimized. These include the required pH for enzymatic and chromogenic reactions, time of incubation of the enzymatic reaction, and the respective concentration of ACh, TMB, and C-AuNPs. Relative absorbance ΔA ($\Delta A = A_0 - A$) was used for the optimization, where A_0 and A is the absorbance at 652 nm in the absence and presence of AChE respectively. (Sec. SI.1 and SI.2)

Assay for AChE activity

50 µL of Tris-HCl buffer (100 mM, pH 7.6), 25 µL of AChE (2 mU·mL^{-1}), and different concentrations of 20 µL acetylcholine chloride (ACh) were mixed and incubated for 20 minutes at 37°C. Then 50 µL of sodium acetate buffer (100 mM, pH 4.0), 25 µL of 0.4 mmol·L^{-1} TMB, 20 µL of C-AuNPs colloidal solution (100 pM), and 20 µL of the above solution were mixed thoroughly. The UV-Vis spectrum of the resultant solution was measured, and the decrease in absorption at 652 nm depicting the aggregation effect of choline as an enzymatic product of AChE activity was measured.

Protocol for PE sensing

The insecticide PE was utilized as a candidate OP that functions by the inhibition of AChE. 50 µL of Tris-HCl buffer (100 mM, pH 7.6), 25 µL of AChE (2 mU·mL^{-1}), and different concentrations of PE (25 µL) were mixed and incubated for 10 minutes at 37°C. Then 20 µL of ACh (4 mmol·L^{-1}) was added to each sample, and the reagents were incubated for an additional 20 minutes. Then, 20 µL of sodium acetate buffer (100 mM, pH 4.0), 25 µL of 0.4 mmol·L^{-1} TMB, 25 µL of C-AuNPs (100 pM), and 20 µL of the above solution were dispensed using a micropipette. The UV-

Vis spectrum of the resultant solution was recorded by an increase in the absorption at 652 nm, which was directly proportional to the concentration of PE.

Since OPs are neurotoxins, all of the experiments were performed under the standard biosafety and chemical safety procedures with appropriate personal protective equipment (PPE).

Authorship contribution statement

Muhammad Musaddiq Shah: Methodology, Investigation, Analysis, and Writing. **Wen Ren:** Conceptualization and Writing. **Bashir Ahmad:** Supervision and Writing. **Joseph Irudayaraj:** Concept, Supervision, and Writing.

Declaration of competing interest

The authors have no known competing financial interests or personal relationships.

References:

1. Shimada, H.; Kiyozumi, Y.; Koga, Y.; Ogata, Y.; Katsuda, Y.; Kitamura, Y.; Iwatsuki, M.; Nishiyama, K.; Baba, H.; Ihara, T. *Sensors and Actuators B: Chemical* **2019**, *298*, 126893.
2. Xiong, S.; Deng, Y.; Zhou, Y.; Gong, D.; Xu, Y.; Yang, L.; Chen, H.; Chen, L.; Song, T.; Luo, A. *Analytical Methods* **2018**, *10* (46), 5468-5479.
3. Songa, E. A.; Okonkwo, J. O. *Talanta* **2016**, *155*, 289-304.
4. Tiwari, N.; Asthana, A.; Upadhyay, K. *Spectrochimica Acta Part A: Molecular and Biomolecular Spectroscopy* **2013**, *101*, 54-58.
5. Pundir, C. S.; Chauhan, N. *Analytical Biochemistry* **2012**, *429* (1), 19-31.
6. Cheng, Z.; Dong, F.; Xu, J.; Liu, X.; Wu, X.; Chen, Z.; Pan, X.; Gan, J.; Zheng, Y. *Food chemistry* **2017**, *231*, 365-373.
7. Behniwal, P. K.; She, J. *International Journal of Environmental Analytical Chemistry* **2017**, *97* (6), 548-562.
8. Muñoz, R.; Guevara-Lara, A.; Santos, J. L.; Miranda, J. M.; Rodriguez, J. A. *Microchemical Journal* **2019**, *146*, 582-587.
9. Guo, Y.; Liu, R.; Liu, Y.; Xiang, D.; Liu, Y.; Gui, W.; Li, M.; Zhu, G. *Science of The Total Environment* **2018**, *613*, 783-791.
10. Liang, B.; Han, L. *Biosensors and Bioelectronics* **2020**, *148*, 111825.

11. Yaseen, T.; Sun, D.-W.; Pu, H.; Pan, T.-T. *Food analytical methods* **2018**, *11* (9), 2518-2527.
12. Weerathunge, P.; Behera, B. K.; Zihara, S.; Singh, M.; Prasad, S. N.; Hashmi, S.; Mariathomas, P. R. D.; Bansal, V.; Ramanathan, R. *Analytica chimica acta* **2019**, *1083*, 157-165.
13. Yan, X.; Li, H.; Han, X.; Su, X. *Biosensors and Bioelectronics* **2015**, *74*, 277-283.
14. Yan, X.; Song, Y.; Wu, X.; Zhu, C.; Su, X.; Du, D.; Lin, Y. *Nanoscale* **2017**, *9* (6), 2317-2323.
15. Zhang, S.-X.; Xue, S.-F.; Deng, J.; Zhang, M.; Shi, G.; Zhou, T. *Biosensors and Bioelectronics* **2016**, *85*, 457-463.
16. Jiang, T.; Song, Y.; Wei, T.; Li, H.; Du, D.; Zhu, M.-J.; Lin, Y. *Biosensors and Bioelectronics* **2016**, *77*, 687-694.
17. Zhang, D.; Chen, Z.; Omar, H.; Deng, L.; Khashab, N. M. *ACS applied materials & interfaces* **2015**, *7* (8), 4589-4594.
18. Ren, W.; Liu, W.; Irudayaraj, J. *Sensors and Actuators B: Chemical* **2017**, *247*, 923-929.
19. Manea, F.; Houillon, F. B.; Pasquato, L.; Scrimin, P. *Angewandte Chemie International Edition* **2004**, *43* (45), 6165-6169.
20. Lin, Z.; Zhang, X.; Liu, S.; Zheng, L.; Bu, Y.; Deng, H.; Chen, R.; Peng, H.; Lin, X.; Chen, W. *Analytica Chimica Acta* **2020**.
21. Cho, I.-H.; Bhunia, A.; Irudayaraj, J. *International journal of food microbiology* **2015**, *206*, 60-66.
22. Huang, Y.; Ren, J.; Qu, X. *Chemical reviews* **2019**, *119* (6), 4357-4412.
23. Cho, I.-H.; Irudayaraj, J. *Analytical and bioanalytical chemistry* **2013**, *405* (10), 3313-3319.
24. Liu, L.; Du, J.; Liu, W.-e.; Guo, Y.; Wu, G.; Qi, W.; Lu, X. *Analytical and bioanalytical chemistry* **2019**, *411* (10), 2189-2200.
25. El Alami, A.; Lagarde, F.; Huo, Q.; Zheng, T.; Baitoul, M.; Daniel, P. *Sensors International* **2020**, 100007.
26. Ma, Y.; Jiang, L.; Mei, Y.; Song, R.; Tian, D.; Huang, H. *Analyst* **2013**, *138* (18), 5338-5343.
27. Atallah, C.; Charcosset, C.; Greige-Gerges, H. *Journal of Pharmaceutical Analysis* **2020**.
28. Ren, W.; Mohammed, S. I.; Wereley, S.; Irudayaraj, J. *Analytical chemistry* **2019**, *91* (4), 2876-2884.
29. Meng, X.; Schultz, C. W.; Cui, C.; Li, X.; Yu, H.-Z. *Sensors and Actuators B: Chemical* **2015**, *215*, 577-583.
30. Guo, J.; Wong, J. X.; Cui, C.; Li, X.; Yu, H.-Z. *Analyst* **2015**, *140* (16), 5518-5525.
31. Colovic, M. B.; Krstic, D. Z.; Lazarevic-Pasti, T. D.; Bondzic, A. M.; Vasic, V. M. *Current neuropharmacology* **2013**, *11* (3), 315-335.
32. Sun, Y.; Tan, H.; Li, Y. *Microchimica Acta* **2018**, *185* (10), 446.
33. Yan, X.; Li, H.; Wang, X.; Su, X. *Talanta* **2015**, *131*, 88-94.
34. Lan, W.; Chen, G.; Cui, F.; Tan, F.; Liu, R.; Yushupujiang, M. *Sensors* **2012**, *12* (7), 8477-8490.
35. Li, X.; Cui, H.; Zeng, Z. *Sensors* **2018**, *18* (12), 4302.
36. Wang, P.; Wan, Y.; Ali, A.; Deng, S.; Su, Y.; Fan, C.; Yang, S. *Science China Chemistry* **2016**, *59* (2), 237-242.

37. Alimentarius, C. International Food Standards. http://www.fao.org/fao-who-codexalimentarius/codex-texts/dbs/pestres/pesticide-detail/en/?p_id=58 (accessed 16-04-2020).
38. Xu, S.; Guo, C.; Li, Y.; Yu, Z.; Wei, C.; Tang, Y. *Journal of hazardous materials* **2014**, *264*, 34-41.
39. Okada, E.; Coggan, T.; Anumol, T.; Clarke, B.; Allinson, G. *Analytical and bioanalytical chemistry* **2019**, *411* (3), 715-724.
40. Xu, Z.-L.; Deng, H.; Deng, X.-F.; Yang, J.-Y.; Jiang, Y.-M.; Zeng, D.-P.; Huang, F.; Shen, Y.-D.; Lei, H.-T.; Wang, H. *Food chemistry* **2012**, *131* (4), 1569-1576.
41. Sun, X.; Gao, C.; Zhang, L.; Yan, M.; Yu, J.; Ge, S. *Sensors and Actuators B: Chemical* **2017**, *251*, 1-8.
42. Yan, X.; Kong, D.; Jin, R.; Zhao, X.; Li, H.; Liu, F.; Lin, Y.; Lu, G. *Sensors and Actuators B: Chemical* **2019**, *290*, 640-647.
43. Dong, P.; Jiang, B.; Zheng, J. *Analytical Methods* **2019**, *11* (18), 2428-2434.
44. Ren, S.; Zhou, F.; Xu, C.; Li, B. *Gold Bulletin* **2015**, *48* (3-4), 147-152.
45. Haiss, W.; Thanh, N. T.; Aveyard, J.; Fernig, D. G. *Analytical chemistry* **2007**, *79* (11), 4215-4221.